

Large-scale electronic structure calculation and its application

Takeo Hoshi

Department of Applied Physics, University of Tokyo, Bunkyo-ku, Tokyo, Japan

e-mail:hoshi@coral.t.u-tokyo.ac.jp, url:fujimac.t.u-tokyo.ac.jp/hoshi/

(Dated: May 22, 2019)

Several methodologies are developed for large-scale atomistic simulations with fully quantum mechanical description of electron systems. The important methodological concepts are (i) generalized Wannier state, (ii) Green function and (iii) hybrid scheme within quantum mechanics. Test calculations are done with upto 10^6 atoms using a standard workstation. As a practical nanoscale calculation, the dynamical fracture of nanocrystalline silicon was simulated.

Keywords large-scale electronic structure calculation, order- N method, generalized Wannier state, Green function, fracture, nanocrystalline silicon.

I. INTRODUCTION

Nanoscale materials are directly governed by quantum mechanical freedoms of electron systems. Nowadays, electron systems of realistic materials are treated by the *ab initio* electronic structure calculations that are based on the density functional theory (DFT)^{1,2}, the first-principle molecular dynamics³, and related theories developed for decades. A typical system size of present *ab initio* calculations is, however, on the order of 10^2 atoms and new practical theories are required for nanoscale calculations. This article is devoted to the methods in large-scale electronic structure calculations and their application to nanoscale materials^{4,5,6,7,8,9}.

In general, a quantum mechanical calculation of an electron system is reduced to an eigen value equation;

$$\hat{H}|\phi_k^{(\text{eig})}\rangle = \varepsilon_k^{(\text{eig})}|\phi_k^{(\text{eig})}\rangle \quad (1)$$

with an effective one-body Hamiltonian \hat{H} . Here the eigen energies and eigen states are denoted as $\{\varepsilon_k^{(\text{eig})}\}$ and $\{\phi_k^{(\text{eig})}\}$, respectively. A physical quantity $\langle \hat{X} \rangle$ is given as

$$\langle \hat{X} \rangle = \sum_k^{\text{occ.}} |\phi_k^{(\text{eig})}\rangle \langle \phi_k^{(\text{eig})}| \hat{X} |\phi_k^{(\text{eig})}\rangle = \text{Tr}[\hat{\rho} \hat{X}] \quad (2)$$

with occupied eigen states $\{\phi_k^{(\text{eig})}\}$ or the one-body density matrix $\hat{\rho}$

$$\hat{\rho} \equiv \sum_k^{\text{occ.}} |\phi_k^{(\text{eig})}\rangle \langle \phi_k^{(\text{eig})}|. \quad (3)$$

The calculation of eigen states, Eq. (1), is usually reduced to a matrix diagonalization procedure and gives a severe computational cost. Therefore, the essential methodology for large-scale calculations is how to obtain the density matrix $\hat{\rho}$ *without calculating eigen states*. This article focuses the methods for structural properties including molecular dynamics simulations. For the above purpose, the most import physical quantity is the total energy¹⁰.

The trace in Eq. (2) is expressed as

$$\text{Tr}[\hat{\rho} \hat{X}] = \int d\mathbf{r} \int d\mathbf{r}' \rho(\mathbf{r}, \mathbf{r}') X(\mathbf{r}', \mathbf{r}) \quad (4)$$

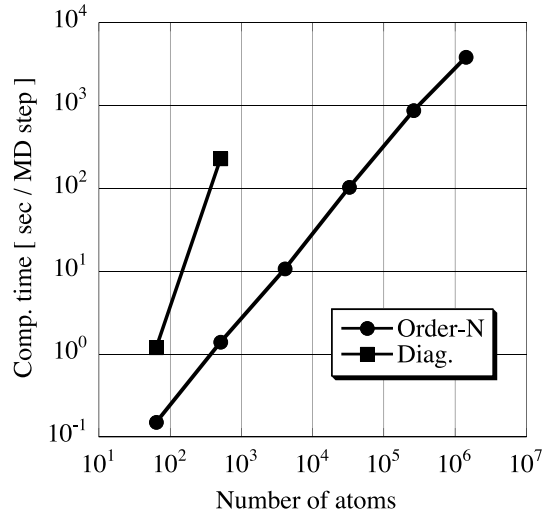


FIG. 1: The computational time of bulk silicon as the function of the number of atoms (N), up to 1,423,909 atoms⁶; The CPU time is measured for one time step in the molecular dynamics (MD) simulation. A tight-binding Hamiltonian is solved using the exact diagonalization method and an ‘order- N ’ method with the perturbative Wannier state (See Section II). We use a standard work station with one Pentium 4TM processor and 2 GB of RAM.

with real space coordinates \mathbf{r}, \mathbf{r}' . The *off-diagonal* components of the density matrix, $\rho(\mathbf{r}, \mathbf{r}')$, $\mathbf{r} \neq \mathbf{r}'$, are essential quantum mechanical freedoms, while the *diagonal* components, the charge density at the point \mathbf{r} ($\rho(\mathbf{r}, \mathbf{r}) \equiv n(\mathbf{r})$), appear also in classical mechanics. As an important fact for practical large-scale calculations, the off-diagonal long range component of the density matrix dose not contribute explicitly to the value of $\langle \hat{X} \rangle$, if the operator \hat{X} is a short range one. We can found a general principle within DFT, called ‘nearsightedness principle’¹², which is directly related to the above fact.

For practical algorithms, there are many proposals. See reviews or comparison papers^{13,14,15,16,17}. In this article, we pick out two typical methods; (i) method with generalized Wannier state and (ii) method with Green function. Figure 1 demonstrates the computational cost

with diagonalization and our calculation⁶. Here one can find that the diagonalization results in a computational cost proportional to N^3 with the system size (N), as is usual in matrix diagonalization procedure ($\propto N^3$). Our calculation, on the other hand, shows an ‘order- N ’ property, with upto 10^6 atoms, in the sense that the computational cost is proportional to the system size ($\propto N$).

II. GENERALIZED WANNIER STATE

The generalized Wannier state is a generalization of the (conventional) Wannier states^{18,19,20} (See Appendix A). Its pioneering works were done by Walter Kohn in the context of large-scale calculations^{21,22}. The pictures of the generalized Wannier states are localized ‘chemical’ wave functions in condensed matter, such as a bonding orbital or a lone-pair orbital, with a slight spatial extension or ‘tail’.

The generalized Wannier states $\{\phi_i^{(\text{WS})}\}$ are defined as localized wave functions that satisfy the equation

$$H|\phi_i^{(\text{WS})}\rangle = \sum_{j=1}^{\text{occ}} \varepsilon_{ij} |\phi_j^{(\text{WS})}\rangle \quad (5)$$

and the orthogonality

$$\langle \phi_i^{(\text{WS})} | \phi_j^{(\text{WS})} \rangle = \delta_{ij}. \quad (6)$$

The matrix ε_{ij} is introduced as the Lagrange multiplier for the constraint of Eq. (6) and is given as

$$\varepsilon_{ij} = \langle \phi_j^{(\text{WS})} | H | \phi_i^{(\text{WS})} \rangle. \quad (7)$$

The solutions of Eq. (5) is equivalent to the unitary transformation of the eigen states $\{\phi_k^{(\text{eig})}\}$

$$|\phi_i^{(\text{WS})}\rangle = \sum_k^{\text{occ.}} U_{ik} |\phi_k^{(\text{eig})}\rangle, \quad (8)$$

where U_{ik} is a unitary matrix. Here the suffix i of the Wannier state $\phi_i^{(\text{WS})}$ denotes its localization center.

It is crucial that the generalized Wannier states reproduce the one-body density matrix $\hat{\rho}$ in Eq. (3), where the eigen states $\{\phi_k^{(\text{eig})}\}$ are replaced by the Wannier states $\{\phi_j^{(\text{WS})}\}$. In results, any physical quantity can be reproduced in the trace form of Eq. (2).²³

The concept of the generalized Wannier state is used for practical large-scale calculations^{4,26,27}. We derived a mapped eigen value equation for the generalized Wannier states

$$H_{\text{WS}}^{(i)} |\phi_i^{(\text{WS})}\rangle = \varepsilon_{\text{WS}}^{(i)} |\phi_i^{(\text{WS})}\rangle \quad (9)$$

with a mapped Hamiltonian $H_{\text{WS}}^{(i)}$ that is dependent on the other Wannier states $\{\phi_j^{(\text{WS})}\}_{j \neq i}$ ^{4,5}. Equation (9) is equivalent to Eqs. (5) and (6). A Wannier state $|\phi_i^{(\text{WS})}\rangle$

is not an eigen state of the original Hamiltonian H but an eigen state of the above mapped Hamiltonian $H_{\text{WS}}^{(i)}$. Equation (9) also shows that the locality of a Wannier state can be mapped, formally, to that of a virtual impurity state⁴.

With Eq. (9), we developed a variational method so as to generate approximate Wannier states, which is called variational Wannier state method⁴. As the practical procedure, Eq. (9) is solved iteratively under explicit localization constraint on each Wannier state

$$\{\phi_i^{(\text{WS})}\} \rightarrow \{H_{\text{WS}}^{(i)}\} \rightarrow \{\phi_i^{(\text{WS})}\} \rightarrow \{H_{\text{WS}}^{(i)}\} \rightarrow \dots \quad (10)$$

With Eq. (9), we also developed a perturbative method to generate Wannier states, which is called perturbative Wannier state method^{4,5}. This method corresponds to a non-iterative solution of Eq. (9). It is noteworthy that the perturbative Wannier state, unlike the variational one, is localized *without any explicit localization constraint*, when a short range Hamiltonian H is used.

III. METHOD WITH GREEN FUNCTION

The large-scale electronic structure calculation can be also formulated by the Green function. The Green function \hat{G} is defined by

$$\hat{G}(\varepsilon + i0^+) \equiv \sum_k \frac{|\phi_k^{(\text{eig})}\rangle \langle \phi_k^{(\text{eig})}|}{\varepsilon + i0^+ - \varepsilon_k^{(\text{eig})}}. \quad (11)$$

The density matrix is calculated by means of energy integration of the Green function;

$$\rho_{ij} = -\frac{1}{\pi} \text{Im} \int G_{ij}(\varepsilon + i0^+) f\left(\frac{\varepsilon - \mu}{k_B T}\right) d\varepsilon. \quad (12)$$

Here, i, j represent atom or orbital index, and f is the Fermi distribution function. The important methodological points are (i) how to calculate the Green function $G_{ij}(\varepsilon + i0^+)$ and (ii) how to calculate the energy integration in Eq. (12). The recursion method gives a solver routine for the Green function without calculating eigen states^{28,29}. As an essence, the approximate Green function is calculated within the limited basis set

$$|i\rangle, \quad H|i\rangle, \quad H^2|i\rangle, \quad \dots H^{n-1}|i\rangle \quad (13)$$

that is constructed from an initial basis $|i\rangle$ ³⁰. In practical large-scale calculations, the number of bases, n , is much smaller than that of the original Hamiltonian matrix H . For example, the number n is chosen to be $n = 40$ as a typical value²⁹.

Recently, we developed a practical Green function method and applied it to molecular dynamics simulations⁸. We also compared the Green function method with the Wannier state method on the resultant density matrix ρ_{ij} ⁸. Now we are planning other molecular dynamics simulations, especially, to metals.

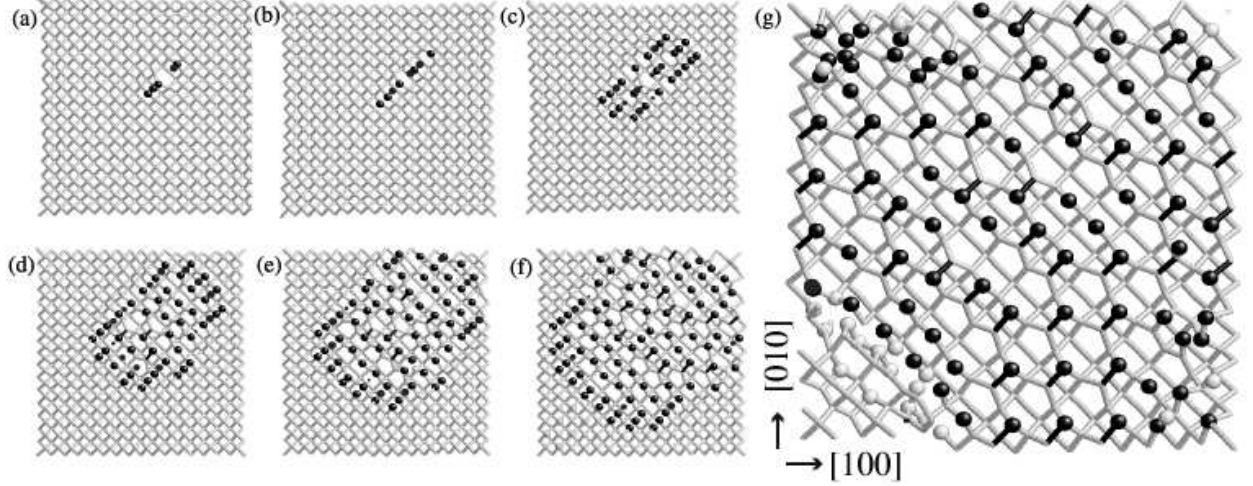


FIG. 2: Snapshots of a fracture process in the (001) plane⁶. The sample contains 4501 atoms and one initial defect bond as the fracture *seed*. The time interval between two successive snapshots is 0.3 ps, except that between (f) and (g) (approximately 1.3 ps). A set of connected black rod and black ball corresponds to an asymmetric dimer. See details in the original paper⁶.

IV. HYBRID SCHEME AND PARALLEL COMPUTATIONS

As another fundamental methodology for large-scale calculations, we developed the hybrid scheme within quantum mechanics^{6,9}. The basic idea is the followings; The one-body density matrix is decomposed into two partial matrices or ‘subsystems’ that are constructed from several occupied wave functions. This decomposition corresponds to dividing the occupied Hilbert space. The *different* partial density matrices are solved by *different* solver methods. Each subsystem is obtained with a well-defined mapped Hamiltonian and a well-defined electron number⁹. Test calculations are done by the combinations between (a) the diagonalization method and perturbative Wannier state methods, (b) the variational and perturbative Wannier state methods⁶ (c) the Green function method and the perturbative Wannier state method⁹. Since the present hybrid scheme is a technique in calculating the density matrix $\hat{\rho}$, any physical quantity is quantum mechanically well defined with Eq. (2).

Parallel computation is also important for large-scale calculations. Test calculation of the perturbative Wannier state method is carried out with upto 10^6 atoms⁷ using the Message Passing Interface technique³¹ and with upto 10^7 atoms⁹ using the OpenMP technique³². We are now developing the parallelization of other methods^{8,9}.

V. APPLICATION AND DISCUSSION

As a practical nanoscale application, the molecular dynamics simulation is performed for fracture of nanocrystalline silicon⁶. A standard workstation is used for the simulations with upto 10^5 atoms. We use the hybrid scheme between the variational Wannier state method

and the perturbative Wannier state method.

In the continuum theory of fracture^{33,34}, a critical crack length is defined by a dimensional analysis between the competitive energy terms of the bulk strain (3D) energy and the surface formation (2D) energy. Since the definition of the critical length is independent on the sample size or the lattice constant, we can expect a crossover in fracture phenomena between nanoscale and macroscale samples. The investigation of the above crossover is one purpose of the present simulation. Another purpose is the fracture behavior in atomistic pictures, on the points of how and why the fracture path is formed and propagates in the crystalline geometry³⁵.

Dynamical fracture processes are simulated under external loads in the [001] direction. As the elementary process in fracture, we observe a two-stage surface reconstruction process. The process contains the drastic change of the Wannier states from the bulk (sp^3) bonding state to surface ones. Figure 2 shows a result, in which the fracture propagates anisotropically on the (001) plane and reconstructed surfaces appear with asymmetric dimers⁶. Step structures are formed in larger systems so as to reduce the anisotropic surface strain energy within a flat (001) surface. Such a step formation is understood as the beginning of a crossover between nanoscale and macroscale samples⁶. Further investigation should be done for direct discussion of the crossover.

The present calculations are carried out using tight-binding Hamiltonian within *s* and *p* orbitals. We should say that its applicability is rather limited, due to the simplicity of Hamiltonian. Its parameter theory, however, reproduces systematically several *ab initio* results among different elements or phases, because the tight-binding formulation is universal within the scaled length and energy units^{4,5,9}. An important future work is to construct simple and practical (tight-binding) Hamiltonians more

systematically from the *ab initio* theory. We will use the muffin-tin orbital formulation for the construction, because it gives directly the tight-binding formulation³⁶.

Recently the concept ‘multiscale mechanics’ is focused as the seamless theoretical connection of material simulation methods among the three principles of mechanics; (I) quantum mechanics (for electron systems), (II) classical mechanics, and (III) continuum mechanics. The present work gives a guiding principle and a typical example for the concept, which is carried out by simplifying the total energy functional.

APPENDIX A: DERIVATION OF CONVENTIONAL WANNIER STATE

Here we derive the conventional Wannier state^{18,20} as a specific case of Eq. (8). In periodic systems, eigen states are called Bloch states $\{\psi_{\nu\mathbf{k}}^{(\text{Bloch})}\}$ with the suffices of the band ν and the \mathbf{k} -point \mathbf{k} , the point in the Brillouin zone.

Within an isolated single band, the Wannier states can be defined $W_{\nu\mathbf{l}}$ with the suffices of the band ν and the lattice vector \mathbf{l} ;

$$W_{\nu\mathbf{l}}(\mathbf{r}) = \int d\mathbf{k} e^{-i\mathbf{k}\mathbf{r}} \psi_{\nu\mathbf{k}}^{(\text{Bloch})}(\mathbf{r}), \quad (\text{A1})$$

where the integration is done within the Brillouin zone³⁷. Equation (8) will be reduced to Eq. (A1), when the corresponding unitary matrix U is chosen as

$$U_{ij} \Rightarrow U_{\nu\mathbf{l},\nu'\mathbf{k}} \equiv \delta_{\nu\nu'} e^{-i\mathbf{k}\mathbf{r}}. \quad (\text{A2})$$

The conventional Wannier state is given by the unitary transform only within an isolated single band ($\nu = \nu'$), while the generalized Wannier states are given by the unitary transform within different bands ($\nu \neq \nu'$). It is also noteworthy that the concept of the generalized Wannier state, unlike the conventional one, can be applicable to non-periodic cases.

¹ P. Hohenberg and W. Kohn, Phys. Rev. **136**, 864 (1964).
² W. Kohn and L. S. Sham, Phys. Rev. **140A**, 1133 (1965).
³ R. Car and M. Parrinello, Phys. Rev. Lett. **55**, 2471 (1985).
⁴ T. Hoshi and T. Fujiwara, J. Phys. Soc. Jpn. **69**, 3773 (2000).
⁵ T. Hoshi and T. Fujiwara, Surf. Sci. **493**, 659 (2001).
⁶ T. Hoshi and T. Fujiwara, preprint (cond-mat 0210366), to appear in J. Phys. Soc. Jpn. **72**, No.10 (2003).
⁷ M. Geshi, T. Hoshi, and T. Fujiwara, preprint (cond-mat/0306461), to appear in J. Phys. Soc. Jpn. **72**, No.11 (2003).
⁸ R. Takayama, T. Hoshi, and T. Fujiwara, in preparation.
⁹ T. Hoshi, R. Takayama, and T. Fujiwara, in preparation.
¹⁰ There also exist large-scale calculation methods for *transport properties*, whose methodological foundation is quite different from the present one. We can find an example¹¹ with the use of the Kubo formula. For review, see the following proceedings of a recent international conference; RIKEN REVIEW **29**, (2000).
¹¹ S. Roche, Phys. Rev. **B59**, 2284 (1999).
¹² W. Kohn, Phys. Rev. Lett. **76**, 3168 (1996).
¹³ P. Ordejón, Comp. Mat. Sci. **12**, 157 (1998).
¹⁴ S. Goedecker, Rev. Mod. Phys. **71**, 1085 (1999).
¹⁵ G. Galli, Phys. Stat. Sol. (b) **217**, 231 (2000).
¹⁶ S. Y. Wu and C. S. Jayanthi, Phys. Rep. **358**, 1 (2002).
¹⁷ D. R. Bowler, M. Aoki, C. M. Goringe, A. P. Horsfield and D. G. Pettifor, Modelling Simul. Mater. Sci. Eng. **5**, 199 (1997).
¹⁸ G. H. Wannier, Phys. Rev. **52**, 191 (1937).
¹⁹ W. Kohn, Phys. Rev. **115**, 809 (1959).
²⁰ See textbooks, such as N. W. Ashcroft and N. D. Mermin, *Solid State Physics*, Saunders College, Philadelphia (1976).
²¹ W. Kohn, Phys. Rev. **B7**, 4388 (1973).
²² W. Kohn, Chem. Phys. Lett. **208**, 167 (1993).
²³ In several papers, the Wannier states are constructed in a post process of the standard electronic structure calculations with eigen states. For silicon crystal, the calculation within DFT was carried out using plane wave bases²⁴ or using muffin-tin orbital bases²⁵. Though their methodologies in constructing Wannier states are quite different, the resultant wave functions show the character of *sp*³ bonding orbital with ‘tail’. The ‘tail’ part of the wave function has node structures on neighbor bond sites, as a consequence of the orthogonality between the Wannier states.
²⁴ N. Marzari and D. Vanderbilt, Phys. Rev. **B56**, 12847 (1997).
²⁵ O. K. Andersen, T. Saha-Dasgupta, and S. Ezhov, Bull. Mater. Sci. **26**, 19 (2003).
²⁶ F. Mauri, G. Galli, and R. Car, Phys. Rev. **B47**, 9973 (1993).
²⁷ P. Ordejón, D. A. Drabold, M. P. Grumbach, and R. Martin, Phys. Rev. **B48**, 14646 (1993).
²⁸ R. Haydock, *The recursive solution of the Schrödinger equaiton*, in *Solid state physics*, ed. H. Ehrenreich, F. Seitz, D. Turnbull **35**, 215 (1980).
²⁹ D. G. Peffifor, Phys. Rev. Lett. **63**, 2480 (1989).
³⁰ The basis set in Eq. (13) is generally called Krylov subspace in mathematical textbooks. See, for example, G. H. Golub and C. F. Van Loan, *Matrix Computations*, third ed., Johns Hopkins University Press, London (1996).
³¹ <http://www.mpi-forum.org/>.
³² <http://www.openmp.org/>.
³³ A. A. Griffith, Philos. Trans. R. Soc. London Ser. A **221**, 163 (1920).
³⁴ As a textbook of fracture, see B. Lawn, *Fracture of brittle solids*, 2nd ed., Cambridge University Press (1993).
³⁵ See Ref.⁶ and references therein.
³⁶ O. K. Andersen, O. Jepsen, and D. Glötzel, in *Highlights of condensed matter theory*, North Holland (1985).
³⁷ In general, Bloch states are not unique with respect to arbitrary phase freedoms ($\phi_{\nu\mathbf{k}}^{(\text{eig})}(\mathbf{r}) \rightarrow \phi_{\nu\mathbf{k}}^{(\text{eig})}(\mathbf{r}) \exp(i\delta_{\nu\mathbf{k}})$). This phase freedom, however, must be properly chosen to construct localized states in Eq. (A1).